Simulated Changes in the Deep Ocean Reservoir of Refractory Dissolved Organic Carbon (DOC) Mediated by Hydrothermal Fluid Fluxes

James Lin[1,2], Timothy DeVries[3], and Robert T. Letscher[1,2]

[1]Department of Earth Sciences, University of New Hampshire, USA

[2]Ocean Process Analysis Laboratory

[3]Department of Geography, University of California, Santa Barbara, USA

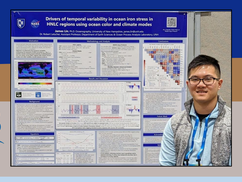

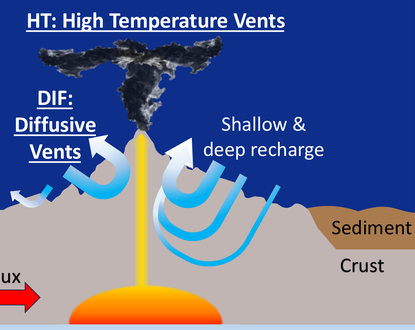

Motivation

- Hydrothermal circulation through the young oceanic crustal and associated DOC source and removal remain poorly constrained processes that could affect the global marine DOC reservoir
- Earth system models require hydrothermal vent fluxes of DOC to better represent the ocean carbon cycle
- **Objective: To simulate global DOC source and removal fields from hydrothermal vents using global seafloor age, fluid fluxes as a function of age, and DOC concentrations**

Background

- Hydrothermal venting occurs in permeable basalts along mid-ocean ridges (MOR) spanning ~60,000 km and ridge flanks ages 0 Myr to 66.4 Myr; decreasing fluid venting flux with lithospheric age
- Three types of venting environments
  - **HT**: high-temperature on-axis (<1 Myr crust and ~250-350°C)
  - **DIF**: diffuse on-axis (<1 Myr crust and <100°C); 50-90% of hydrothermal heat loss; 90-95% of seawater
  - **OFF**: off-axis flanks (1-66.4 Myr crust) across abyssal plains
- Based on *in situ* observations from Juan de Fuca Ridge axis, HT removes ~20 µM DOC (by thermal oxidation of refractory DOC (RDOC)), DIF adds ~10-15 µM DOC (by chemosynthesis to semi-labile DOC (SLDOC) or abiotic reduction of CO_2), and OFF removes ~1-4 µM DOC (by sorption and heterotrophic consumption) (Lang et al., 2006).
  - SLDOC- cycles on months to years (15 yr euphotic, 6 yr below euphotic), RDOC- cycles on decades to millennia (16,000 yr)

Methods

A. Interpolate the age of oceanic lithosphere (*Figs. 1 & 2*) based on magnetic polarity age estimates of the seafloor into a new grid for modeling in CESMv2-MARBL grid (Community Earth System Model version 2- Marine Biogeochemistry Library)
B. Derive the fluid flux of the seafloor based on hydrothermal fluid flux as a function of age (Table 1: Johnson and Pruis, 2003)
C. Divide the fluid flux by volume (m^3) of last grid cell for each column to derive annual **fluid flux rate** (yr^{-1}: *Fig. 3*)
D. Compute global **DOC source flux for DIF (0-1 Myr**) vs **DOC removal flux for HT and OFF (0-66.4 Myr)**
E. Three simulations (CESMv2-MARBL) using last 20-yr average of 310 yr simulations (291-310 yr)
   1. $Vent_{source}$ model: For DIF at 0-1 Myr seafloor age, multiply fluid flux rate by 15 µM DOC (15 x10^{-3} mol/m^3), split into 90% SLDOC and 10% RDOC, then add to the last grid cell.
   2. $Vent_{removal}$ model: For HT and OFF at 0-66.4 Myr seafloor age, multiply fluid flux rate by RDOC concentration at last grid box for vent removal, then subtract from RDOC concentration in the last grid cell.
   3. $Vent_{off}$ model: No model changes
F. Calculate DOC vent source and removal (*Tables 2-5*)
G. Plot maps and section plots (100°W & -17.6°S) (*Figs. 4-9*)

$$DOC\ Vent\ Source = Vent_{source} - Vent_{off}$$

$$DOC\ Vent\ Removal = Vent_{off} - Vent_{removal}$$

Research Questions: How much DOC is added or removed by hydrothermal vents? What is the net DOC from vents? What is the spatial distribution of vent DOC sources and removal?

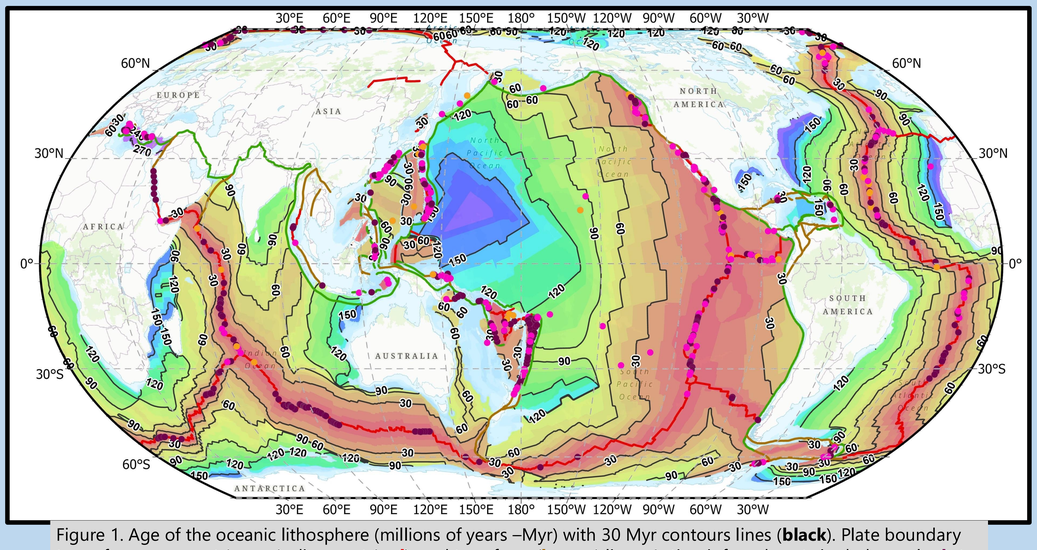

Figure 1. Age of the oceanic lithosphere (millions of years –Myr) with 30 Myr contours lines (**black**). Plate boundary types for convergent (**green**), divergent (**red**), and transform (**brown**) lines. Active, inferred vents in dark purple **dots**, active confirmed vents in light purple **dots**, and inactive vents in orange **dots**. Red is the youngest crust (0 Mya) vs purple is oldest crust (280 Mya) (Müller et al., 2008). ~60% of Earth is underlain by oceanic crustal lithosphere with ages ranging from 0 Myr to 280 Myr. Map created in ArcGIS Pro, using graticules from Equal Earth Projection.

Table 1. Hydrothermal fluid flux from crustal reservoir as a function of seafloor age.

Age (Myr)	Fluid Flux (10^9 m^3/yr)
0-1	2,443
1-4.8	594
4.8-9.7	879
9.7-14.1	337
14.1-18.9	579
18.9-23.4	505
23.4-28	492
28-32.6	430
32.6-38.5	403
38.5-45.3	155
45.3-51.8	87
51.8-58.6	85
58.6-66.4	54
>66.4	0

Total Hydrothermal fluid flux

Johnson and Pruis (2003)
- 0-65 Myr: 7.1x10^{12} m^3/yr
- 0-5 Myr: 2.3x10^{12} m^3/yr
- 5-65 Myr: 4.8x10^{12} m^3/yr

This study
- 0-66.4 Myr: 7.042x10^{12} m^3/yr
- 0-1 Myr: 2.443 x10^{12} m^3/yr
- 1-66.4 Myr: 4.6x10^{12} m^3/yr

Interpolated Seafloor Age

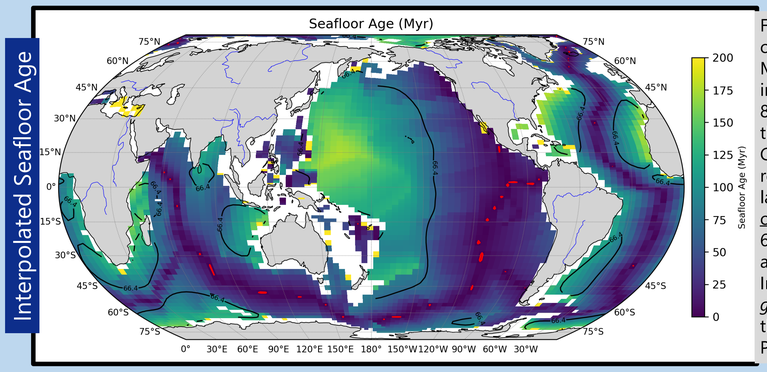

Figure 2. Seafloor crustal age (Myr) from Müller et al. (2008) interpolated from 8,640 x 10,800 grid to the 3° horizontal CESMv2-MARBL grid resolution (116x100: lat x lon). Black contour lines mark 66.4 Myr, and red dots are 0-1 Myr crust. Interpolation used *griddata* function in the SciPy library for Python 3.12.4.

Age-Dependent Seafloor Fluid Flux Rate

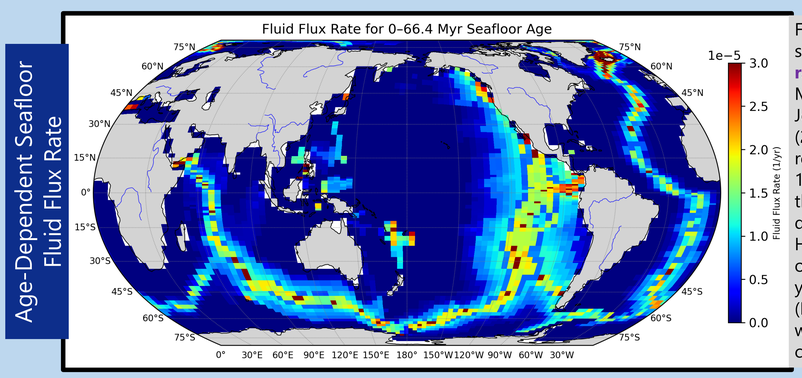

Figure 3. Global seafloor **fluid flux rate** (yr^{-1}) for 0-66.4 Myr crust, based on Johnson and Pruis (2003) age-flux relationship (Table 1) normalized by the volume of the deepest grid cell. Higher fluid rates occur along younger lithosphere (MOR) and diminish with increasing crustal age.

DOC Vent Source

Table 2. Global total DOC source from vents (Pg C). Difference=$Vent_{source}$-$Vent_{off}$

	$Vent_{source}$	$Vent_{off}$	Difference
Global SLDOC	20.87	20.84	0.0278
Global RDOC	601.59	601.49	0.0998
Global total DOC	622.46	622.33	0.1275

Table 3. Annual DOC produced from vents. Production equals difference from Table 2 divided by 310 simulation years.

	Difference (Tg)	Production (Tg/yr)
Global SLDOC	27.8	0.0897
Global RDOC	99.8	0.322
Global total DOC	127.5	0.411

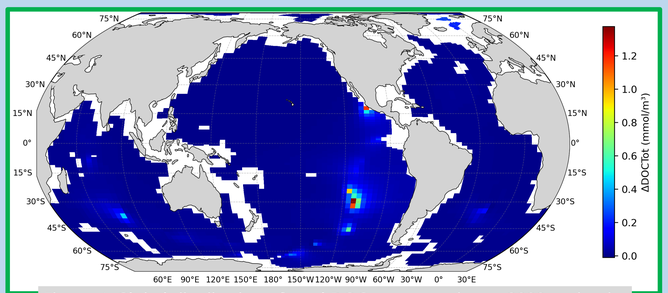

Figure 4. Global distribution of total DOC concentration at 2889 m depth. Results are shown for concentration differences between $Vent_{source}$-$Vent_{off}$.

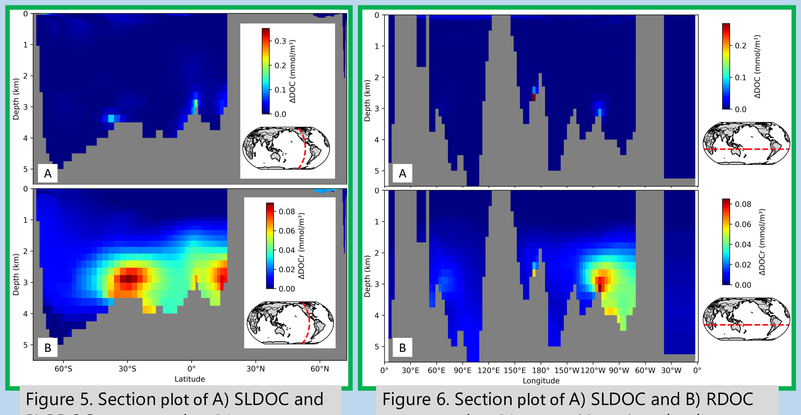

Figure 5. Section plot of A) SLDOC and B) RDOC concentration ($Vent_{source}$-$Vent_{off}$) vs depth at 100°W.

Figure 6. Section plot of A) SLDOC and B) RDOC concentration ($Vent_{source}$-$Vent_{off}$) vs depth at -17.6°S.

DOC Vent Removal

Table 4. Total DOC removal from vents (Pg C). Difference=$Vent_{off}$-$Vent_{removal}$. *Minus added to signify DOC loss at hydrothermal vents.

	$Vent_{off}$	$Vent_{removal}$	*Difference
Global SLDOC	20.83262	20.8325	-0.00012
Global RDOC	604.65575	604.58606	-0.06969
Global DOC	625.48838	625.41856	-0.06981

Table 5. Annual DOC removed by vents. Removal equals difference from Table 4 divided by 310 simulation years.

	Difference (Tg)	Removal (Tg/yr)
Global SLDOC	-0.012	-0.000387
Global RDOC	-69.69	-0.2248
Global total DOC	-69.81	-0.225

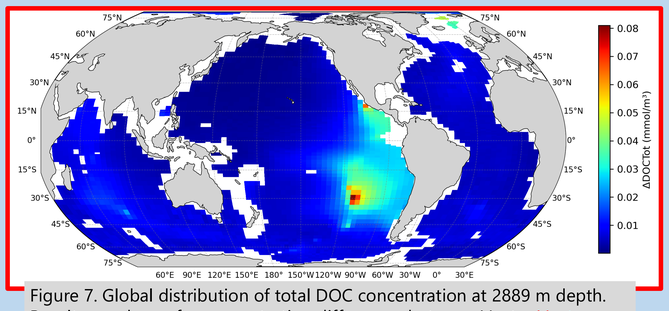

Figure 7. Global distribution of total DOC concentration at 2889 m depth. Results are shown for concentration differences between $Vent_{off}$-$Vent_{removal}$.

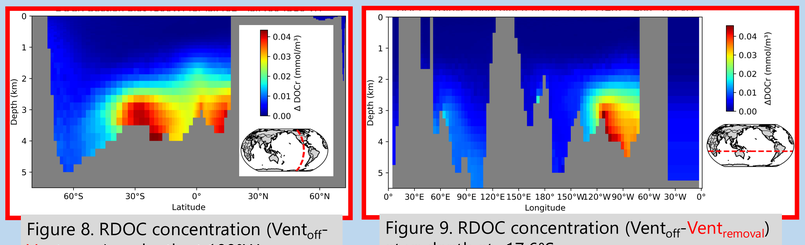

Figure 8. RDOC concentration ($Vent_{off}$-$Vent_{removal}$) vs depth at 100°W.

Figure 9. RDOC concentration ($Vent_{off}$-$Vent_{removal}$) at vs depth at -17.6°S.

Results

- Estimates of hydrothermal fluid flux and carbon are dependent on seafloor age and heat loss partitioned between HT, DIF, and OFF vents at 0-66.4 Myr crust
- Global fluid flux=7.042x10^{12} m^3/yr vs 7.1×10^{12} m^3/yr (Johnson & Pruis, 2003) vs 20 × 10^{12} m^3/yr (Coogan & Gillis, 2018)
  - Global river flux= 37x10^{12} m^3/yr (*~5x more than vents*)
- **DIF model simulates 9x more preaged SLDOC added at seafloor 0–1 Myr than RDOC, but only vent RDOC accumulates and gets transported 1-2 km above the vents**
  - Total DOC flux at 15 uM (0-1 Myr) = 0.411 Tg DOC/yr
    - 0.0897 Tg SLDOC/yr and 0.322 Tg RDOC/yr
      - 0.03-0.28 Tg DOC/yr (Lang et al., 2006)
  - Global river flux = 173 Tg DOC/yr (*>400x more than vents*)
- **HT and OFF vents remove deep sea RDOC**
  - -0.225 Tg RDOC/yr
- **Net 0.1 Tg RDOC/yr (0.322-0.225) added by hydrothermal vents, but isotope δ^{13}C-DOC and radiocarbon Δ^{14}C-DOC composition will change between vents and deep ocean**
  - **Vent δ^{13}C-DOC=−30‰** vs deep ocean δ^{13}C-DOC=−21‰
  - **Vent Δ^{14}C-DOC = −800‰ (13,000 yr)** vs deep ocean Δ^{14}C-DOC = -400 to -530 ‰ (4,000 to 6,000 yr)
- **Caveats**: (**1**) DOC concentrations are from a single vent site (Juan de Fuca Ridge), (**2**) vent DOC bioavailability is poorly constraint (90% SLDOC & 10% RDOC partition at DIF), (**3**) particle-iron scavenging of RDOC at HT is not represented, (**4**) hydrothermal plume temperature, salinity, and other tracer fluxes are not simulated, and (**5**) model resolution (~90,000 km^2) is 5 orders magnitude larger than real plumes (~0.1 km^2)

Conclusions

Acknowledgements

- This research was supported by the National Science Foundation (NSF) under Grant No. 2049590.
- Computations were performed on Marvin, a Cray CS500 supercomputer at UNH supported by the NSF MRI program under grant AGS-1919310.
- Data source: https://www.ngdc.noaa.gov/mgg/ocean_age/data/2008/grids/age/

References

- Bemis, K., Lowell, R., & Farough, A. (2012). Diffuse Flow On and Around Hydrothermal Vents at Mid-Ocean Ridges. *Oceanography*, *25*(1), 182–191. https://doi.org/10.5670/oceanog.2012.16
- Bradley, D.C., 2008. Passive margins through earth history. Earth-Science Reviews, 91(1-4), pp.1-26.
- Coogan, L. A., & Gillis, K. M. (2018). Low-Temperature Alteration of the Seafloor: Impacts on Ocean Chemistry. *Annual Review of Earth and Planetary Sciences*, *46*(1), 21–45. https://doi.org/10.1146/annurev-earth-082517-010027
- Druffel, E. R. M., & Griffin, S. (2015). Radiocarbon in dissolved organic carbon of the South Pacific Ocean. *Geophysical Research Letters*, *42*(10), 4096–4101. https://doi.org/10.1002/2015GL063764
- **Johnson, H. P., & Pruis, M. J. (2003). Fluxes of fluid and heat from the oceanic crustal reservoir. *Earth and Planetary Science Letters*, *216*(4), 565–574. https://doi.org/10.1016/S0012-821X(03)00545-4**
- **Lang, S. Q., Butterfield, D. A., Lilley, M. D., Paul Johnson, H., & Hedges, J. I. (2006). Dissolved organic carbon in ridge-axis and ridge-flank hydrothermal systems. *Geochimica et Cosmochimica Acta*, *70*(15), 3830–3842. https://doi.org/10.1016/j.gca.2006.04.031**
- **Muller, R. D., M. Sdrolias, C. Gaina, and W. R. Roest (2008), Age, spreading rates, and spreading asymmetry of the world's ocean crust, Geochem. Geophys. Geosyst., 9, Q04006, https://doi.org/10.1029/2007GC001743**
- Virtanen, P., Gommers, R., Oliphant, T. E., Haberland, M., Reddy, T., Cournapeau, D., Burovski, E., Peterson, P., Weckesser, W., Bright, J., van der Walt, S. J., Brett, M., Wilson, J., Millman, K. J., Mayorov, N., Nelson, A. R. J., Jones, E., Kern, R., Larson, E., Carey, C. J., Polat, İ., Feng, Y., Moore, E. W., VanderPlas, J., Laxalde, D., Perktold, J., Cimman, R., Henriksen, I., Quintero, E. A., Harris, C. R., Archibald, A. M., Ribeiro, A. H., Pedregosa, F., van Mulbregt, P., & SciPy 1.0 Contributors. (2020). SciPy 1.0: Fundamental Algorithms for Scientific Computing in Python. Nature Methods, 17(3), 261-272. DOI: 10.1038/s41592-019-0686-2.